J Mater Sci (2007) 42:9663–9670
DOI 10.1007/s10853-007-1947-5

SAXS observation of RCM1 under cyclical shear

Daniel T. Cooney · Jonathan P. DeRocher · Geoff D. Moggridge · Adam M. Squires

Received: 5 October 2006 / Accepted: 19 June 2007 / Published online: 30 July 2007

Abstract A cylinder forming poly(styrene-*b*-butadiene-*b*-styrene) triblock copolymer melt is cyclically processed through a capillary at a high shear rate in the Cambridge Multipass Rheometer (MPR). In situ X-ray diffraction experiments enable observation of the effect of the shear on the block copolymer (BCP) nanophase orientation, both during and after processing. Temporal resolution of the X-ray exposures is increased, whilst retaining intensity, by exploiting the cyclical nature of the shear and the material's response to it; short exposures from many cycles, individually having few counts, are added together to produce well resolved X-ray patterns. Orientation of the cylinders reduces during processing, then increases during pauses between processing. The loss of orientation is attributed to the high shear rate deforming the melt faster than the structure can respond, whilst it is believed that melt relaxation, linked to the compressibility of the material, produces much lower shear rates after mechanical processing has ceased, which induces strong orientation of the nanostructure.

D. T. Cooney · J. P. DeRocher · G. D. Moggridge
Department of Chemical Engineering, University of Cambridge, New Museums Site, Pembroke Street, Cambridge CB2 3RA, UK

D. T. Cooney
e-mail: dtc24@cam.ac.uk

J. P. DeRocher
e-mail: jd377@cam.ac.uk

G. D. Moggridge
e-mail: gdm14@cam.ac.uk

A. M. Squires (✉)
Department of Chemistry, The University of Reading, PO Box 224, Whiteknights, Reading RG6 6AD, UK
e-mail: a.m.squires@reading.ac.uk

Introduction

Block copolymers

This investigation describes the observation of phase orientation in a cylinder-forming block copolymer (BCP) experiencing high shear rates, using a laboratory X-ray source. BCP molecules are composed of chemically distinct polymer chains, covalently bonded together to form a single macromolecule. Below the order–disorder transition temperature, mixing of separate BCP components is unfavourable but the inter-block covalent bonds prevent macroscopic phase separation, forcing local phase separation to occur [1–3]. The resultant phase morphologies depend upon both the block and overall molecule length, with characteristic dimensions typically of the order of 10–100 nm. BCP phase separation has been widely investigated and is especially well documented in the case of the simple two component diblock and ABA triblock systems [e.g., 1]. RCM1 is an SBS triblock copolymer forming a cylindrical poly(butadiene) phase in a matrix of poly(styrene).

Keller [4] first observed shear ordering in an extruded lamellar BCP, and BCP phase orientation is still the subject of much research, both experimental [e.g., 5] and theoretical [e.g., 6]. Most work examining shear ordering in polymer melts uses moderate shear rates, up to about 100/s, to encourage phase orientation. Higher shear rates have been applied to polymers in solution—for instance Harada et al. [7] reached extrusion shear rates of 1,700/s. More recently [8] the effects of high shear rates, up to 1,020/s, on block copolymer micelles in aqueous solutions have been observed during processing using SAXS and small angle light scattering.

One area that remains unclear is the effect of shear on the order–disorder transition (ODT), the point at which

phase segregation becomes less favourable than mixing. This is most often characterised by the ODT temperature, T_{ODT}, above which the material is disordered, and below which segregation occurs.

Winter et al. [9] reported that large amplitude oscillatory shear (LAOS) (with a low frequency of 0.01 rad/s) at 10 °C below the quiescent T_{ODT} of a cylinder-forming SIS triblock suppressed phase segregation, although at lower temperatures the shear was seen to improve ordering. They explain this finding on the basis that the applied shear can disrupt segregation (in an analogous way to thermal energy) and so a lower temperature is required to promote disorder when shear is present. Conversely other studies [e.g., 10, 11] investigated higher shear rates (in the range 6 to 30/s) up to 20 °C above the quiescent T_{ODT} and established that the shear encouraged phase segregation. In a more recent review [12], shear is accepted as increasing T_{ODT} with reference to work from the Bates group [13, 14]. No mention is made of Winter's earlier findings, although the paper is considered elsewhere in the review. This observed shear-elevating of T_{ODT} remains unexplained, although an analogous effect has been observed in lamellar to Multi Lamellar Vesicle transitions in concentrated surfactants [15, 16].

Balsara and Dai [17] investigated a cylinder forming SI diblock in solution, finding they could induce order above the ODT at modest shear rates, but that higher shear rates reduced the ordering again. They interpret their results in terms of a relaxation time for fluctuations in the phase structure; if this relaxation time is much larger than the reciprocal shear rate then the structure cannot respond to the shear, resulting in disordering of the structure. At lower shear rates, ordering is induced as the molecular motions can respond on the timescale of the shear. This is consistent with theoretical work predicting an increase in T_{ODT} with shear [18, 19].

Multipass rheometer

The Multipass Rheometer (MPR) is a double-piston capillary rheometer developed at the University of Cambridge [20], which allows for a small sample of fluid to be processed back and forth many times at high shear rates whilst monitoring the pressure drop across the capillary. The MPR also has integrated temperature control up to 200 °C, making it suitable for testing polymer melts. MPR3 has been constructed to allow simultaneous processing and X-ray observation of a sample, utilising an effectively X-ray transparent beryllium capillary, and has been previously used to observe flow-induced polymer crystallisation [21] and the structure of detergent micelles [16]. A two-dimensional detector is used to record the X-ray scattering, allowing observation of both diffraction angle and phase orientation.

These previous applications of this system have yielded good results in the WAXS domain. It can also be operated in SAXS mode, with a maximum sample to detector distance of around 77 cm. However, the need for tighter beam collimation imposed by the need to observe small angle diffraction patterns results in a reduced X-ray flux (due to pin-hole collimation) for SAXS experiments compared to WAXS.

X-ray diffraction

X-ray diffraction occurs in BCP samples due to the difference in electron density between the two phase domains, resulting in small angle diffraction indicative of the repeat distances in the phase morphology. Since the electron density difference is not large in many BCP systems (including this one), where both blocks contain only carbon and hydrogen, the diffraction is relatively weak.

Aligned cylindrical domains in a BCP will diffract to positions perpendicular to the cylinder axis, forming a two spot/lobe pattern—the tighter the lobes, the greater the orientation. Unaligned but phase separated samples will exhibit diffraction to the same scattering vector, but in a full circle (like a powder diffraction pattern). In order to assess the quality of orientation it is necessary to have a method of quantifying the extent of orientation from a 2D diffraction pattern.

Such quantification can be achieved using a 2D analogue, F, of the 3D order parameter suggested by de Gennes [22]. By integrating around the azimuthal angle, χ, at a given scattering vector, the observed intensity, $I(\chi)$, can be normalised to give a distribution function, $f(\chi) \cdot d\chi$, where

$$f(\chi) = \frac{I(\chi)}{\int_0^{\pi} I(\chi) d\chi} \tag{1}$$

The single numerical parameter, F, describing this distribution is defined as

$$F = \left\langle 1 - 2\cos^2 \chi \right\rangle = \int_0^{\pi} f(\chi)\left(1 - 2\cos^2 \chi\right) \cdot d\chi \tag{2}$$

This formulation is similar to that used elsewhere in the literature [23, 24], but is multiplied by a factor of –1, since we define χ to be zero at the position of the beam stop stem, which is parallel to the flow direction. This results in preferential scattering to $\chi = \pi/2$ rather than $\chi = 0$ or π.

The combination of low X-ray flux (imposed by the equipment) and weak diffraction (due to the sample) leads to long collection times required to obtain satisfactory

diffraction patterns from the system. This results in a loss of time resolution, and hence the ability to probe different points in a fast processing cycle.

To compensate for this problem, this study examines the application of a method for improving the time resolution. This method involves taking many short X-ray exposures over many repetitions of the same experiment. This concept lends itself neatly to processing in the MPR, so long as it can be established that each cycle is the same (i.e., extended processing doesn't produce a physical change in the fluid). In post-processing, frames taken at the same point in the experiments/processing cycles are added together.

Experimental

A triblock copolymer consisting of two poly(styrene) blocks separated by a poly(butadiene) block, called RCM1, was provided by BASF. RCM1 is approximately 74% by volume poly(styrene), forming a nanostructure of poly(butadiene) rods in a poly(styrene) matrix below its quiescent T_{ODT} at >220 °C. The molecular weight, M_n, is around 100,000 g/mol and M_w/M_n is about 1.2. The polymer was processed at 170 °C in MPR3. All processing was conducted in a beryllium capillary of diameter 2 mm, which was close to the optimum sample thickness for X-ray scattering based on electron density calculations [25]. All processing was carried out at a piston velocity of 5 mm/s, which corresponds in this experimental set up to a shear rate of ~1,100/s.

X-ray diffraction of material processed in the MPR, through a beryllium capillary 2 mm in diameter and 10 mm long, was made possible by a custom built Bruker GADDS system. Cu $K\alpha$ X-rays were generated at 45 kV and 45 mA. Small angle diffraction was recorded using a crossed wire, 2D detector.

Continuous exposures were taken for 600 s. Processing conditions for the exposures are denoted by three numbers e.g., '5-5-18': the first indicating MPR piston velocity in mm/s, the second indicating the processing amplitude in mm, and the third indicating the pause in seconds between passes. These conditions are prefixed by 'D' or 'A', to indicate if the exposure was taken during processing, or after processing was ceased.

Composite image collections were made by a novel method outlined by the flow diagram in Fig. 1. During MPR processing a series of 5 s exposures were taken over many cycles, started simultaneously with the pistons moving after a pause section in the cycle. These individual exposures each contained very few counts, but were stamped with the time they were taken. After collection, this time was compared with the log file generated by the MPR, which notes the change in position of the pistons with time. This allowed each exposure to be allocated to a position in the processing cycle. Once this was done for all exposures, the cycle itself was divided into 5 s time frames and those exposures allocated to the same frame were combined. For the purpose of this paper all data is standardised to a total collection time of 600 s.

The validity of this experimental approach depends on the material changing cyclically during the piston strokes, but not undergoing longer timescale changes over many piston strokes. This is demonstrated by the consistency over the duration of the composite collection experiments of both the pressure profiles for each piston stroke (Fig. 2), and the averaged X-ray patterns recorded over a number of piston strokes (Fig. 3).

Steady shear experiments were conducted using a Rheometrics Scientific ARES rheometer, using 25 mm parallel plates and a sample thickness of approximately 1.5 mm, lasting for 20 min at 170 °C.

Results and discussion

Continuous collection

The melt was processed in multipass mode in the MPR with a piston velocity of 5 mm/s, over an amplitude of 5 mm (providing a 10 mm full pass), with a pause between passes of 18 s (conditions denoted '5-5-18'). This gave an overall cycle length (consisting of two passes in opposite directions and two pauses) of 40 s. Continuous collections of 600 s were made during processing ('D 5-5-18'), and for the 600 s directly after the 600 s of processing was ceased ('A 5-5-18'). In addition a collection was made whilst processing with only a 1 s pause ('D 5-5-1').

RCM1 had previously been identified as having a primary scattering peak at $2\theta = 0.37°$. Alignment of the phase domains was expected to show as diffraction lobes at azimuthal angles, χ, of 90° and 270°, perpendicular to the direction of shear.

Figure 4 shows radial integrals of the diffraction data as a function of azimuthal angle χ. Whilst there is clearly preferential diffraction to the expected angle of 90° in the 'A 5-5-18' exposure (with the highest integrated peak intensity and $F = 0.34$), there is less orientation evident in the exposure taken during the processing (D 5-5-18) ($F = 0.21$), and very little at all (very weak peak and $F = 0.16$) in the exposure with the shorter pause time (D 5-5-1)

Composite collection

The continuous experiments showed a trend of decreasing orientation (F-value) with increased fraction of time spent

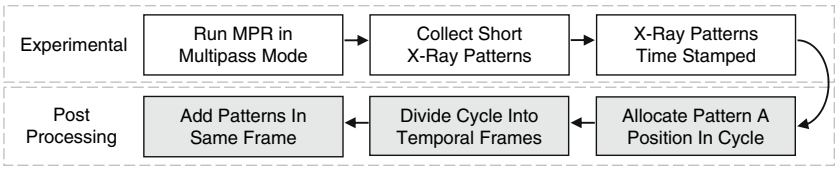

Fig. 1 Flow diagram for composite frame collection and production

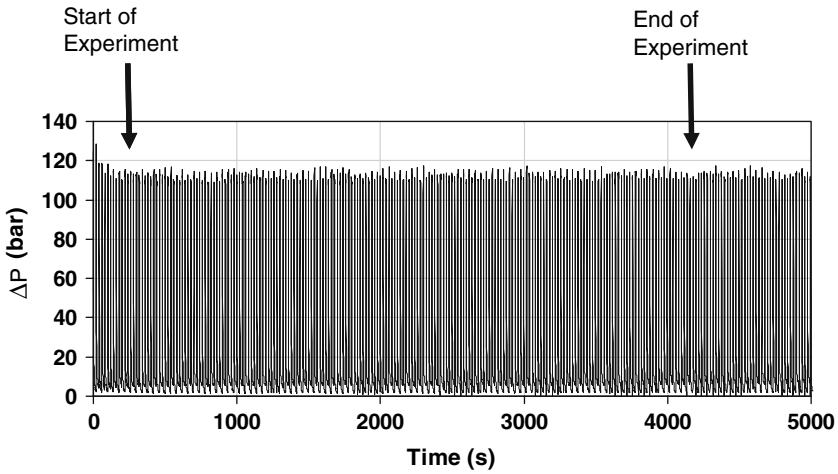

Fig. 2 Pressure differences across the test section over the course of the composite experiment 5-5-18. The start and end of the recording of composite frame X-ray data are indicated

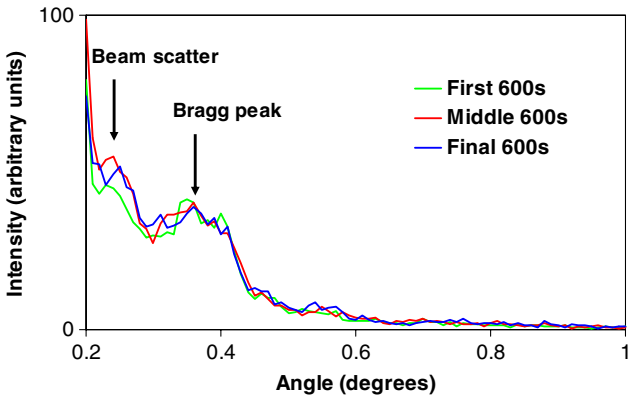

Fig. 3 "Average" X-ray patterns at the start of, during, and at the end of the composite frame experiment 5-5-18. Patterns were constructed by adding up successive frames to produce 600 s of almost continuously recorded X-ray data (in fact the data is not quite continuous because there is a small pause between each 5 s frame of X-ray data). Data is integrated between $\chi = 70$ and 110°

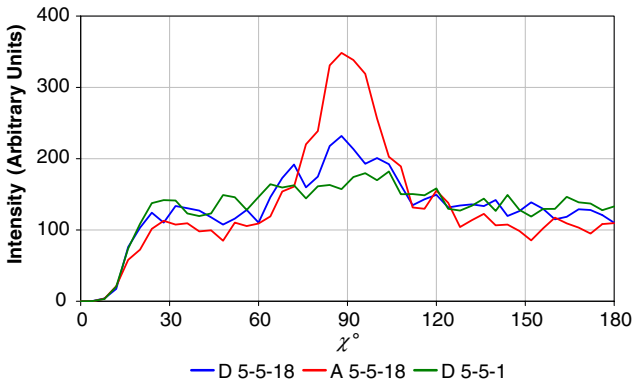

Fig. 4 SAXS diffraction integrals for RCM1 under different processing conditions. Continuous 600 s exposures, showing preferential scattering at $\chi \sim 90°$ (beam stop located at 0°). Integrals taken from $2\theta = 0.3$–0.5 rads, spanning principle diffraction peak at $2\theta = 0.37$ rads. Experiment labels start with 'D' to indicate an exposure taken during processing or 'A' to indicate an exposure taken after processing is ceased, followed by the processing piston velocity in mm/s, the pass amplitude in mm, and the pause between passes in seconds

processing. The oriented diffraction appeared to develop after processing was ceased, but in order to evaluate this better, enhanced time resolution was required. Due to the low count detection rate, using shorter continuous exposures to probe the processing at greater time resolution would not yield useful results.

The scheme outlined in Fig. 1 was devised to observe the increase in diffraction over time. It had been observed that there was no apparent change in macroscopic properties of the sample with processing—each cycle produced similar pressure drops implying similar rheology. It is reasonable to infer from this that the microscopic properties/structures vary in the same way over each cycle. Based on this supposition, exposures lasting 5 s were taken whilst processing (at 5-5-18) was in progress. Collection of the first frame coincided with the onset of motion of the pistons after a rest period. Since the overall cycle lasted 40 s, 8 exposures were taken per cycle. After many cycles, exposures taken at the same point of the cycle were added

together to produce a composite diffraction frame for each of the eight sections of the cycle.

The 2D X-ray patterns and the maximum values of the integrated intensities (over the range $2\theta = 0.3$–0.5) are plotted in 5. An increase in peak integrated intensity reflecting an increase in sample alignment can be observed over the first four frames. The intensity then drops, coinciding with the movement of the pistons before another increase over the last four frames. Although the first and second half of the data represent a different processing direction, the data for each direction are similar, as would be expected from the symmetry of the geometry. A similar trend is observed in F, which ranges from 0.15 to 0.25. Subsequent figures plot F rather than the peak integrated intensity, which provides a more rigorous measure of the extent of alignment, but is independent of the total amount of scattering. The maximum integrated intensity allows direct comparison between continuous and composite experiments, allowing the validity of the composite collection technique to be verified. Intensity data for the continuous exposures (represented by the horizontal lines in the figure) are shown alongside the data for the composite frames in Fig. 5.

The continuous 'D 5-5-18' exposure was expected to be the time average of these eight frames, and this proved to fit very well. The composite frame peak intensities and orientation factors are not as high as those observed in the 'A 5-5-18' experiment, indicating that the orientation continues to develop beyond 18 s after processing ceases. Also, none of the data points are as weak as the 'D 5-5-1' case, supporting the earlier observation that exposures involving more processing show lower peak intensities.

These observations, taken together, confirm the earlier supposition that the structure is varying in the same way for every pass through the rheometer, validating the experimental technique.

The 'A 5-5-18' experiment showed that a higher orientation factor could be achieved than had been obtained in any of the individual frames. A further set of composite frames were produced for a cycle incorporating a longer pause of 38 s (5-5-38). The frame length was maintained at 5 s, so the entire cycle of 80 s comprised 16 frames. Once again, the data matches well with the time averaged continuous collections (not shown), with the data for the first 20 s after each piston motion also in good agreement with the previous experiment.

Figure 6 shows the orientation factor for each frame obtained for the 5-5-38 cycle. The trend for increasing F with time since processing continues but the orientation doesn't significantly improve on what was observed in the shorter experiment, ranging from 0.13 to 0.26. However, at this point F was still not as large as for the continuous 'A 5-5-18' exposure (or 'A 5-5-38'—not shown here), implying the phase ordering was still not completed.

This experiment also allows for a calculation of the maximum observed error in our orientation factor, which will derive in the main part from the low number of counts being recorded. If we expect both processing directions to be equivalent, we can compare the orientation factors from the first half-cycle of the 'D 5-5-18' experiment with those

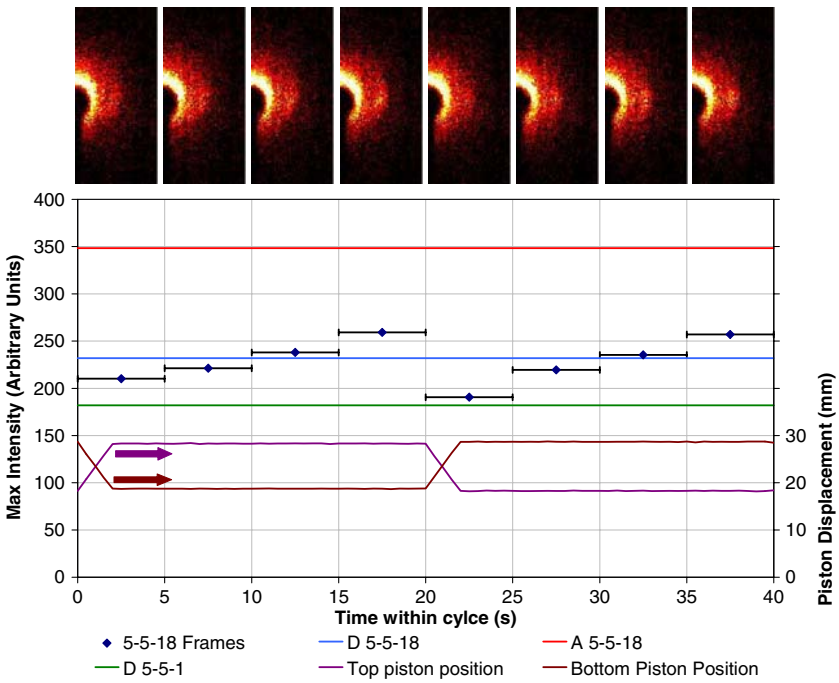

Fig. 5 Top: 2D SAXS patterns for each composite frame. Below: Maximum integrated intensity in each composite frame, with 'error' bars to show extent of frame. Also shown are guides for the maximum intensities from previously mentioned continuous exposures, and MPR piston positions (read from secondary axis) to elucidate frame data. Experiment labels start with 'D' to indicate an exposure taken during processing or 'A' to indicate an exposure taken after processing is ceased, followed by the processing piston velocity in mm/s, the pass amplitude in mm, and the pause between passes in seconds

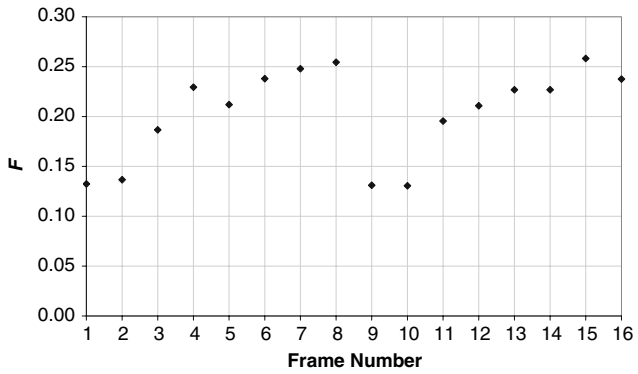

Fig. 6 Orientation factor, F, for composite frames obtained during processing with piston velocity of 5 mm/s, a pass amplitude of 5 mm and a pause between passes of 38 s to give a 40 s total cycle length

in the second. We would also expect to see the same pattern in the first four frames of the 'D 5-5-38' experiment, as well as frames 9 to 12 (the first 4 frames after processing in the opposite direction). Such comparison reveals a maximum disparity of 0.06 between data points, giving a maximum error of ±0.03. This is not insignificant, but is smaller than the overall changes in F factor being observed.

A further composite frame experiment extended the processing pause further to 598 s, to give 1,200 s for a full processing cycle. Exposures were collected for 60 s, with the first exposure, as before, starting with the start of piston movement. However, in this case, since previous experiments had shown little difference between processing directions, and to minimise the required processing time, the frames were combined not only with other frames from the same point in the cycle, but also frames that were out of phase by π. This resulted in 10 composite frames. Figure 7 shows the orientation factors for these frames, alongside those for the first eight '5-5-38' frames.

The two series compare well. The first point in the '5-5-598' series, representing an average of the first 60 s in a cycle, has an orientation factor within the range of the '5-5-38' series, and the next point is beyond this range, as would be expected. The subsequent data show a slightly increasing trend, but it is clear that the orientation factor isn't changing very much in the final few frames. In fact, after 4 min, the orientation factor is over 90% of the final value of $F = 0.32$, which is within the calculated error of the value of $F = 0.34$ observed in the experiment where the data were acquired directly after processing (A5-5-18).

To distinguish whether the degree of phase separation is changing during these tests it is necessary to examine the total counts in the 2θ range of interest. Since this value could be distorted by the presence of the beam stop, the counts in one quarter of the range (from $\chi = 90$ to 180°) are examined, which, through symmetry, should equal one quarter of the total intensity over all azimuthal angles. Figure 8 presents this data for all three processing conditions studied using this composite frame method. Very little variation is observed in the total counts for any of the three series. Compared to the 5-5-598 experiment there tends to be a higher intensity for the 5-5-38 frames and a lower intensity for the 5-5-18 frames, but this variation is most likely due to slight variations in configuration introduced by reloading the MPR (requiring the X-ray enclosure to be moved).

If the BCP phase structure was completely destroyed by the shear, we would expect to see a lower value of the total counts during shear and an increase in total counts after shear ceased (and phase separation occurs again). Since little variation of the total counts is observed, this would imply that the diffracting phase structure is still present, but not aligned.

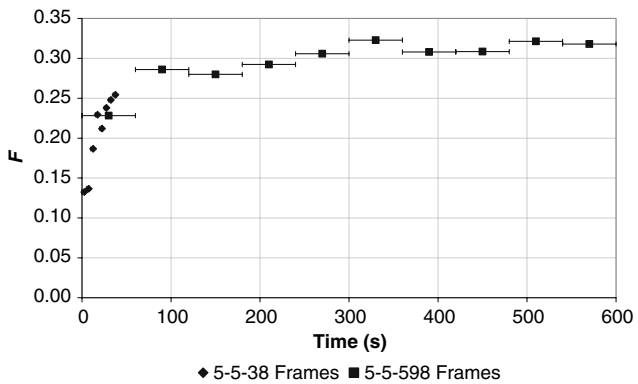

Fig. 7 Orientation factor, F, for composite frames obtained during processing, plotted against time since onset of piston movement. 'Error' bars show extent of collection for each frame. Experiment labels show the processing piston velocity in mm/s, the pass amplitude in mm, and the pause between passes in seconds

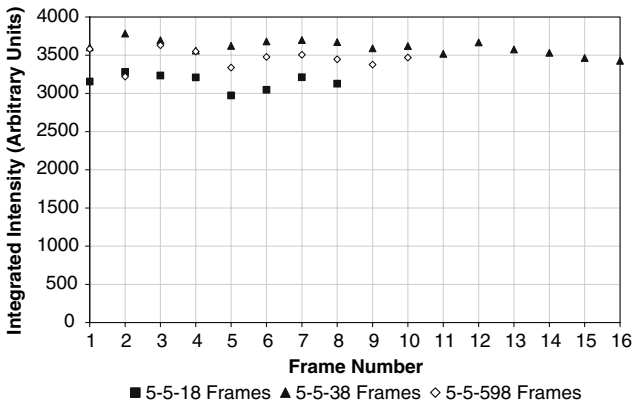

Fig. 8 Total counts in one quarter ($90 < \chi \leq 180$) of the diffraction 'rings' for composite frames produced at different operating conditions. Experiment labels show the processing piston velocity in mm/s, the pass amplitude in mm, and the pause between passes in seconds

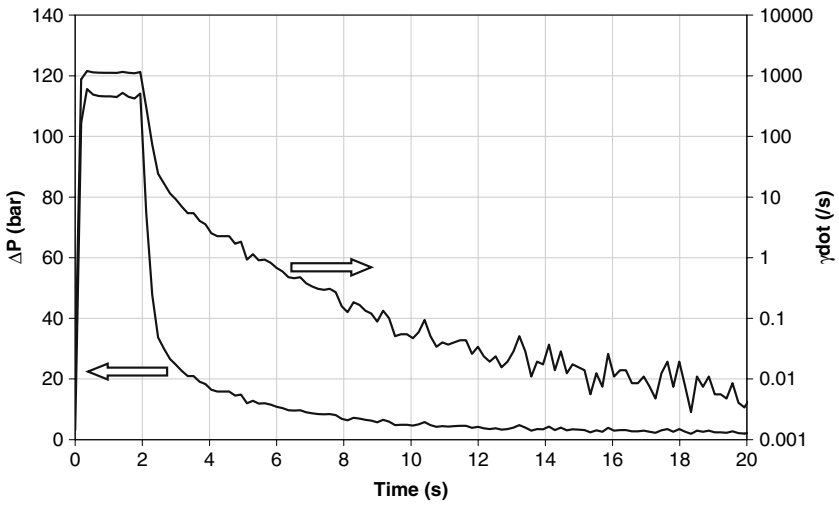

Fig. 9 Pressure trace across a 2 mm capillary and the derived apparent wall shear rate for RCM1 being processed with a piston velocity of 5 mm/s, a pass amplitude of 5 mm and a pause between passes of 18 s to give a 20 s total cycle length

Low shear experiments

Figure 9 shows the pressure drop across the capillary, and the derived apparent wall shear rate, for a '5-5-18' cycle. Although the shear rate is extremely high during the processing, the slightly compressible nature of the melt causes a slow pressure equalisation after processing is halted. This relaxation produces much lower shear rates that are experienced during the processing pause [26]. Given the evidence in the literature for shear orientation, it is believed that these shear rates are responsible for the phase alignment after processing ceases.

In order to confirm the effect of low shear rates on the domain orientation, a sample was subjected to a steady shear of 0.1/s in the ARES at the same temperature as the MPR experiments. SAXS was performed on the sample before and after the shear.

Before shear the disc, made by compression moulding, shows little alignment. After shear, there is clear orientation, with intense scattering at 90° to the direction of flow throughout the disc and an orientation factor of $F = 0.55$ at the disc rim.

Unfortunately, attempts to repeat the steady shear experiment at higher shear rates were unsuccessful, due to the limitations of the rheometer. Conversely, to produce shear rates as low as 0.1/s in the MPR would require piston speeds of less that 0.005 mm/s—beyond the limit of reliable control.

Conclusions

A novel X-ray collection procedure has greatly increased the temporal resolution of a lab-based X-ray source, allowing for useful data to be collected from material processed in an MPR.

In situ X-ray experiments have shown loss of phase orientation in a triblock copolymer undergoing extremely high shear, well below its quiescent T_{ODT}, whilst lower shear rates have been shown to improve phase orientation. Following high shear in a capillary, which causes the destruction of phase orientation, slow recovery of orientation is observed. This is attributed to much lower shear rates being generated as the material in the rheometer relaxes. This process is entirely repeatable and can be replicated over a very large number of shear cycles, showing that the structures generated are equilibrium ones.

It is believed this is the first such observation for a BCP melt. However, it is believed the behaviour can be explained in terms of pre-existing theories on BCP phase behaviour—particularly that of Balsara and Dai [17] which allows for shear-induced loss of order when shear rates are so high that the polymer can't respond quickly enough to the changing environment.

References

1. Bates FS (1991) Science 251:898
2. Hamley IW (2001) J Phys: Condens Matter 13:R643
3. Matsen MW, Bates FS (1996) Macromolecules 29:7641
4. Keller A, Pedemonte E, Willmouth FM (1970) Colloid Polym Sci 238:385
5. Boker A, Schmidt K, Knoll A, Zettl H, Hansel H, Urban V, Abetz V, Krausch G (2006) Polymer 47:849
6. Fraser B, Denniston C, Muser MH (2006) J Chem Phys 124:104902
7. Harada T, Bates FS, Lodge TP (2003) Macromolecules 36:5440
8. Castelletto V, Hamley IW (2006) Polym Adv Technol 17:137
9. Winter HH, Scott DB, Gronski W, Okamoto S, Hashimoto T (1993) Macromolecules 26:7236
10. Bates FS, Koppi KA, Tirrell M, Almdal K, Mortensen K (1994) Macromolecules 27:5934
11. Nakatani AI, Morrison FA, Douglas JF, Mays JW, Jackson CL, Muthukumar M (1996) J Chem Phys 104:1589

12. Castelletto V, Hamley IW (2004) Curr Opin Colloid Interface Sci 8:426
13. Koppi KA, Tirrell M, Bates FS (1993) Phys Rev Lett 70:1449
14. Almdal K, Mortensen K, Koppi KA, Tirrell M, Bates FS (1996) J Phys II 6:617
15. Mckeown SA, Mackley MR, Moggridge GD (2003) Trans IChemE Part A 81:649
16. Liaw MS, Mackley MR, Bridgwater J, Moggridge GD, Bayly AE (2003) AIChE J 49:2966
17. Balsara NP, Dai HJ (1996) J Chem Phys 105:2942
18. Cates ME, Milner ST (1989) Phys Rev Lett 62:1856
19. Marques CM, Cates ME (1990) J Phys—Paris 51:1733
20. Mackley MR, Marshall RTJ, Smeulders J (1995) J Rheol 39:1293
21. Mackley MR, Moggridge GD, Saquet O (2000) J Mater Sci 35:5247, 10.1023/A:1004824924912
22. de Gennes PG (1975) In: The physics of liquid crystals. Oxford University Press, London, p 23
23. Clemons CM, Giacomin AJ, Caulfield DF (1998) In: Conference proceedings at Antec '98: Plastics on my mind, Atlanta, p 1432
24. Spahr DE, Friedrich K, Schultz JM, Bailey RS (1990) J Mater Sci 25:4427, 10.1007/BF00581104
25. Cullity BD (1978) In: Elements of X-Ray diffraction. Addison-Wesley, Reading (Massachusetts), p 13
26. Ranganathan M, Mackley MR, Spitteler PHJ (1999) J Rheol 43:443